Research Article / Araştırma Makalesi GU J Sci, Part A, 9(3): 299-313 (2022) https://doi.org/10.54287/gujsa.1160449

Gazi University
Journal of Science
PART A: ENGINEERING AND INNOVATION
http://dergipark.org.tr/gujsa

Molecular Docking, HOMO-LUMO, Quantum Chemical Computation and Bioactivity Analysis of vic-Dioxim Derivatives Bearing Hydrazone Group Ligand and Their Ni^{II} and Cu^{II} Complexes

Şerife Gökçe ÇALIŞKAN[1*], Onur GENÇ[1], Fatma EROL[2], Nursabah SARIKAVAKLI[3]

[1]*Aydin Adnan Menderes University, Faculty of Sciences and Arts, Department of Physics, 09010, Aydin, TURKIYE*
[2]*Gazi University, Technical Sciences Vocational School, Ostim, 06374, Ankara, TURKIYE*
[3]*Aydin Adnan Menderes University, Faculty of Sciences and Arts, Department of Chemistry, 09010, Aydin, TURKIYE*

Keywords

vic-dioxim
Hydrazones
Molecular Docking
HOMO-LUMO
Bioactivity

Abstract

Molecular docking process was performed to investigate the interactions between the synthesized compounds and human epidermal growth factor protein kinase domain EGFR (PDB ID:1M17) and cyclin-dependent kinase-2 CDK2 (PDB ID:3IG7) proteins. HOMO LUMO orbital energy analysis, quantum chemical calculations were made and the bioactivity parameters of the compounds were evaluated. Ni^{II} and Cu^{II} complexes of the L^1H_2 L^2H_2 and L^3H_2, ligands showed higher binding affinity to EGFR and CDK2. Especially, $[Cu(L^1H)_2]$ and $[Cu(L^2H)_2]$ complexes can be suggested as hit compounds against CDK2 and EGFR, respectively. These were supported by the inhibition constant values which were the lowest when compared to others. L^1H_2 L^2H_2 and L^3H_2, ligands had the lowest binding energy values when compared to metal complexes. Also, $[Cu(L^2H)_2]$ complex had a high binding energy value against EGFR. $[Ni(L^2H)_2]$ and $[Cu(L^2H)_2]$ complexes with EGFR had the highest LE and FQ values and these were found to be in the recommended range. Furthermore, $[Cu(L^3H)_2]$ had an acceptable FQ value however its LE value was out of range. Besides, $[Cu(L^2H)_2]$ had a potent and sufficient electrophile ability (acceptor) among other compounds. In conclusion, these compounds may be suitable compounds for further analysis in anti-cancer drug development with low toxic and targeted properties.

Cite

Caliskan, S. G., Genc, O., Erol, F., & Sarikavakli, N. (2022). Molecular Docking, HOMO-LUMO, Quantum Chemical Computation and Bioactivity Analysis of vic-Dioxim Derivatives Bearing Hydrazone Group Ligand and Their Ni^{II} and Cu^{II} Complexes. *GU J Sci, Part A*, *9*(3), 299-313.

Author ID (ORCID Number)

Ş. G. Çalışkan, 0000-0001-5421-3472
O. Genç, 0000-0002-9061-7519
F. Erol, 0000-0002-4103-0148
N. Sarikavakli, 0000-0002-9359-7672

Article Process

Submission Date 10.08.2022
Revision Date 22.09.2022
Accepted Date 26.09.2022
Published Date 29.09.2022

1. INTRODUCTION

In recent years, transition metal complexes carrying vic-dioxime ligands have been the subject of intense studies due to their applications in many scientific fields such as coordination chemistry, biomedicine and electrochemistry. The interaction of a central metal with surrounding ligands (atoms, ions or molecules) has been a major area of interest in coordination chemistry (Rija et al., 2011). From the beginning 1905s vic-dioximes have been used widely as chelating agents in coordination chemistry (Tschugaeff, 1907; Canpolat & Kaya, 2005). vic-dioximes and hydrazones are interesting objects because of their wide application in medicine, industry and analytical chemistry. vic-dioxim derivatives act as amphoteric ligands due to the presence of weakly acidic -OH groups and basic -C=N groups. Therefore, they can form highly stable complexes with most of the transition metals in the periodic table (Serin, 2001, Smith et al., 2003, Kurtoglu & Baydemir, 2007).

Compounds bearing hydrazone and/or oxime linkage attracted the attention of many scholars because of their ability to form stable metal complexes with various transition metals, in addition to the presence of N–OH

*Corresponding Author, e-mail: gcaliskan@adu.edu.tr

moiety, which could enhance their chelation ability and make it more flexible in the reduction, oxidation, and conjugation with organic and inorganic compounds.

These compounds also play an important role in fields such as stereochemistry., structure isomerism, spectroscopy, a model for biological system, cation exchange and ligand exchange chromatography, analytical reagents, as well as catalysts in various chemical processes (Soga et al., 2001; Park et al., 2005).

New anti-cancer drug development studies are gaining more importance day by day and the studies in this field are increasing rapidly. There are proteins responsible for cancer cell development, proliferation and differentiation, which are important targets that must be inhibited by newly synthesized compounds. For example, epidermal growth factor receptor (EGFR), vascular endothelial growth factor receptor (VEGFR), cyclin-dependent kinase-2 (CDK2) are responsible for the growth, nutrition and proliferation of tumour cells (Haider et al., 2021). Various studies have been conducted experimentally and theoretically to investigate the effects of newly synthesized compounds against these target proteins (Altamimi et al., 2021; Horchani et al., 2021; Fouad & Adly, 2021). For instance, Horchani et al. (2021) investigated the inhibitory effects of synthetic pyrazolo-primidinones tethered with hydrazide-hydrazones on EGFR by means of molecular docking and cell viability and Fouad and Adly (2021) reported the molecular docking results of Cu^{2+} and Zn^{2+} nanocomplexes against CDK2 cancer target protein. However, in these studies, quantum chemical calculations of the compounds were not performed and their bioactivity was not analyzed. Literature search reveals that there are no reports based on molecular docking, HOMO-LUMO, quantum chemical computation and bioactivity analysis on hydrazone group-bearing vic-dioxim derivatives and their metal complexes against cancer target proteins EGFR and CDK2. Because of this scarcity observed in the literature, we wanted to reveal the effects of vic-dioxim derivatives carrying the hydrazone group and their metal complexes against cancer target proteins EGFR and CDK2 by molecular docking, HOMO-LUMO, quantum chemical computation and bioactivity analysis.

In the present work, three unsymmetric vic-dioxim derivatives bearing the hydrazone group and their metal complexes with Ni^{II} and Cu^{II} metal ions which were synthesized by us for the first time in our previous study (Sarikavakli & Cakici, 2012) were investigated by means of HOMO-LUMO, quantum chemical computation, bioactivity analysis and molecular docking against the target cancer proteins EGFR and CDK2.

2. MATERIAL AND METHOD

In this study, our starting material, anti-glyoxime hydrazine, (GH_2), which was synthesized and brought to the literature by us for the first time in our previous study, was synthesized with anti-chlorglyoxime and hydrazine hydrate (Sarikavakli & Irez, 2005).

According to the literature; anti-glyoxime hydrazine ,(GH_2), was prepared by reported procedures vic-dioxime ligands containing the hydrazone group, anti-p-hydroxybenzaldehydeglyoxime hydrazone (L^1H_2); (1Z,2E)-N'-[(E)-(2,3-dihydroxyphenyl)methylidene]-2-(hydroxyimino)ethanehydroximohydrazide; (L^2H_2); (1Z,2E)-2-(hydroxyimino)-N'-[(E)-(2-hydroxy-3-methoxyphenyl)methylidene]ethanehydroximohydrazide, (L^3H_2) have been prepared from (1Z,2E)-2-(hydroxyimino)ethanehydroximohydrazide, p-hidroksibenzaldehit, o-pyrocatechualdehyde or o-vanillin. Mononuclear [$M(L^1H)_2$, $M(L^2H)_2$ and $M(L^3H)_2$], where $M=Ni^{II}$ and Cu^{II} complexes of the bidentate ligands were synthesized according to the literature (Sarikavakli & Cakici, 2012) (Figure 1-4).

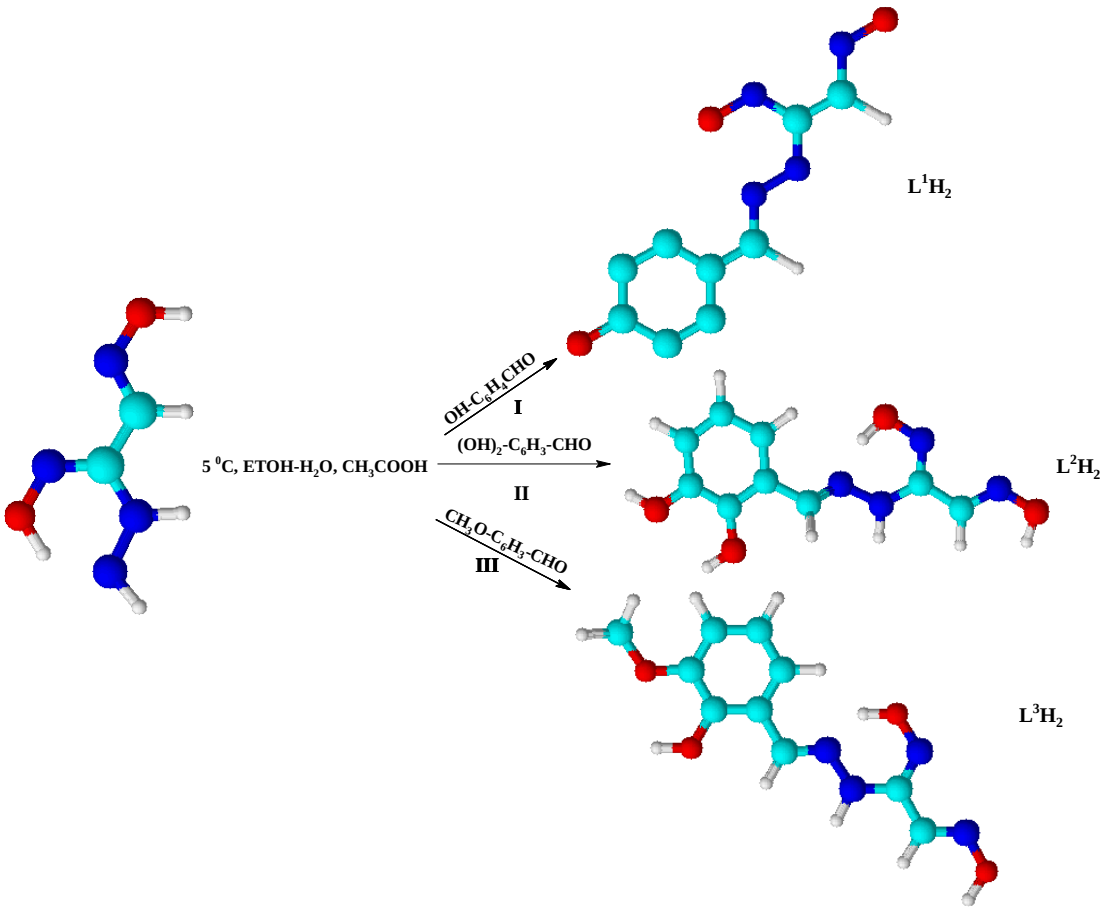

Figure 1. *Chemical structures of ligands*

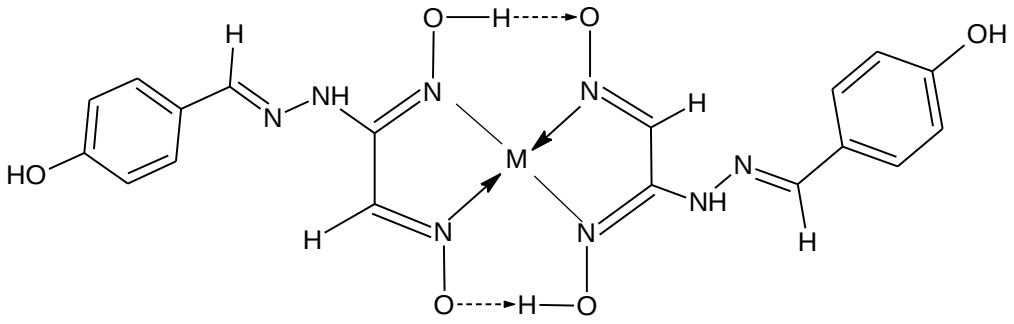

Figure 2. *Complexes of expected structures of the ligand [L^1H_2]*

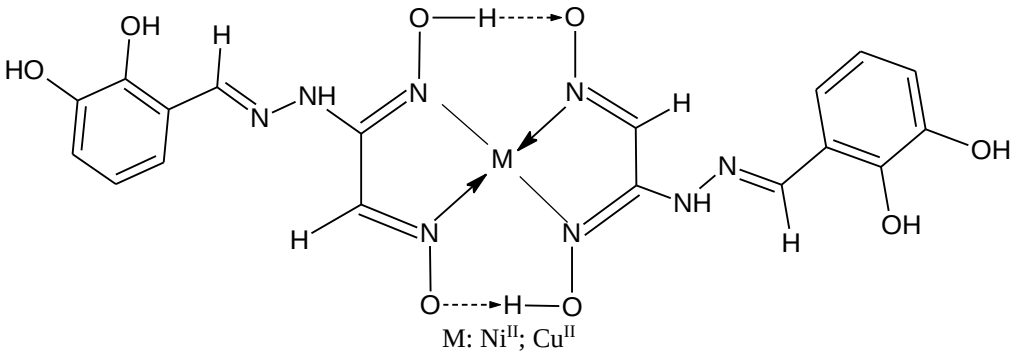

Figure 3. *Complexes of expected structures of the ligand [L^2H_2]*

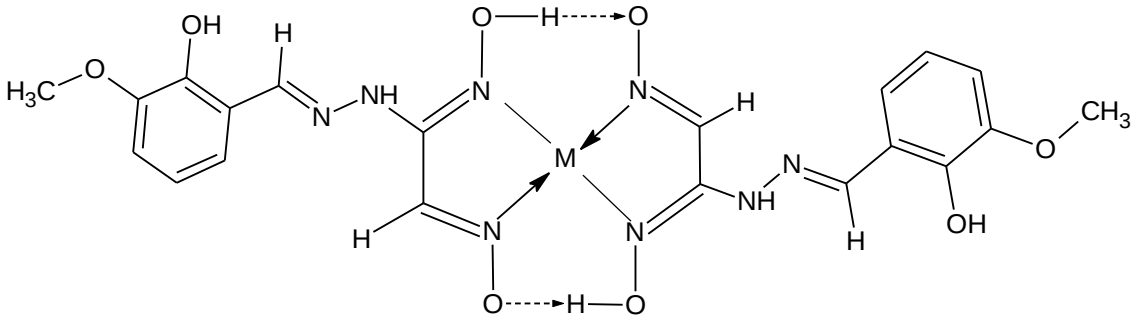

M: Ni^{II}; Cu^{II}

Figure 4. *Complexes of expected structures of the ligand [L^3H_2]*

2.1. Molecular Docking Studies

2.1.1. Protein preparation

Epidermal growth factor protein kinase domain EGFR (PDB ID:1M17) and cyclin-dependent kinase-2 CDK2 (PDB ID:3IG7)'s 3-D structures were obtained from Protein Databank (https://www.rcsb.org/). The preparation process includes the deletion of water molecules, polar hydrogen atom addition and Kollmann charge addition and is performed by using Autodock tools 1.5.7 software (ADT, The Scripps Research Institute, La Jolla, CA, USA). The prepared protein was saved in PDBQT format finally.

2.1.2. Ligand preparation

2-D ligand and metal complex structures were sketched by ChemSketch software. The optimization process was performed by Avogadro v1.2.0 software and the final forms of the compounds were converted into 3-D and saved in pdb format. The setting of torsion tree and the rotatable and non-rotatable bounds present in the ligand was performed by using Autodock tools 1.5.7 software (ADT, The Scripps Research Institute, La Jolla, CA, USA). They were saved in PDBQT format.

2.1.3. Molecular docking

Autodock Vina (Trott & Olson, 2009) was used for molecular docking of the synthesized compounds against target proteins EGFR and CDK2. Grid values were adjusted by Autogrid utility of AutoDock software so as to cover the target protein. Its size was set to 100 Å × 100 Å × 100 Å by 0.375 Å separation. The interactions that occurred between the compounds and target proteins were visualized by PyMol (DeLano, 2013) and DS visualizer software (Accelrys, 2014).

Inhibition constant (K_i) values of the compounds were reached by means of equation (1) where Gibbs free energy (ΔG) was obtained from the docking process, R is the gas constant (R = 1.99 cal/mol K) and T is the absolute temperature (298.15 °K). Low K_i value indicates the potency of being a hit compound.

$$K_i = 10^{(\Delta G \div RT)} \tag{1}$$

2.4. Ligand Bioactivity

For the discovery of a potent compound, a candidate for a novel drug, the affinity parameter is insufficient, there must be evaluated the bioactivity properties of the compound also. The most preferred ligand bioactivity parameters are called ligand efficiency (LE) and fit quality (FQ) and are calculated by equations (2)-(4).

$$LE = -\frac{\Delta G}{HA} \tag{2}$$

$$LE_{scale} = 0.873e^{-0.026\times HA} - 0.064 \quad (3)$$

$$FQ = LE \div LE_{scale} \quad (4)$$

2.5. Quantum Chemical Descriptors

The molecules' geometry optimization was performed by using the Density Functional Theory (DFT) method with B3LYP functional and a basis set of 6-31G. Afterward, the ORCA input files were created by Avogadro v1.2.0 software. Highest occupied molecular orbital (HOMO) and lowest unoccupied molecular orbital (LUMO) were extracted from ORCA output file directly and IboView (Knizia, 2022) was used to visualize the structure of the molecules in detail. The difference between HOMO and LUMO values was calculated according to equation (5).

$$\Delta E_{gap} = |E_{HOMO} - E_{LUMO}| \quad (5)$$

According to Koopmans' theorem (Koopmans, 1934) the initial ionization energy (I) and electron affinity (A) are approximately equal to the minus values of HOMO and LUMO, respectively. Moreover, electronegativity (χ), chemical potential (π), global hardness (η), global softness (σ), and global electrophilicity (ω) were calculated according to equations (6-10) (Koopmans, 1934).

$$\chi = \frac{1}{2}(\mathrm{I} + \mathrm{A}) \quad (6)$$

$$\eta = \frac{1}{2}(\mathrm{I} - \mathrm{A}) \quad (7)$$

$$\pi = -\frac{1}{2}(\mathrm{I} + A) \quad (8)$$

$$\sigma = \frac{1}{\eta} = \frac{2}{(I - A)} \quad (9)$$

$$\omega = \frac{\chi^2}{2\eta} \quad (10)$$

3. RESULTS AND DISCUSSION

3.1. Chemistry

In this study, vic-dioxime ligands containing the hydrazone group were obtained according to the method specified in the literature (Sarikavakli & Irez, 2005; Sarikavakli & Cakici, 2012). Synthesis of the target compounds was achieved using 1:1 molar ratios (Figure 1). The target compounds anti-glyoxime hydrazine, (GH_2), and benzaldehyde derivatives in absolute ethanol at 25^0C gave three substituted (1*Z*,2*E*)-2-(hydroxyimino)ethanehydroximohydrazide (L^1H_2); (L^2H_2) and (L^3H_2).

The ligands (L^1H_2); (L^2H_2) and (L^3H_2) were complexed with divalent (Ni^{II} and Cu^{II}) metal salts to yield mononuclear complexes corresponding to the general formula ML_2 (Sarikavakli & Irez, 2005).

3.2. Molecular Docking

L^1H_2, L^2H_2, L^3H_2 ligands and their Ni^{II} and Cu^{II} metal complexes were docked with target proteins EGFR and CDK2 to evaluate the interactions. Table 1 includes the binding energy and inhibition constant values. Interactions types that occurred between the compounds and target protein molecules were also depicted in Table 2 in detail.

Our results include four types of H bond interactions as conventional hydrogen bond, carbon-hydrogen bond, salt bridge and pi-donor hydrogen bond, four types of hydrophobic interactions as alkyl, pi-alkyl, pi-sigma, pi-pi stacked and three types of electrostatic interactions as attractive charge, pi-anion and pi-cation interactions in Table 2.

***Table 1**. Binding energy (affinity) and inhibition constants of the compounds with target proteins of EGFR (PDB ID: 1M17) and CDK2 (PDB ID: 3IG7)*

Compound	Target Protein	Binding Affinity (kcal/mol)	Inhibition Constant μM
L^1H_2	1M17	-6.4	0.014
	CDK2	-5.2	0.010
$[Ni(L^1H)_2]$	1M17	-7.5	0.008
	CDK2	-7.2	0.013
$[Cu(L^1H)_2]$	1M17	-7.0	0.019
	CDK2	-7.7	0.006
L^2H_2	1M17	-6.4	0.014
	CDK2	-5.5	0.063
$[Ni(L^2H)_2]$	1M17	-8.3	0.008
	CDK2	-7.2	0.013
$[Cu(L^2H)_2]$	1M17	-8.9	0.003
	CDK2	-7.6	0.007
L^3H_2	1M17	-6.3	0.016
	CDK2	-5.7	0.045
$[Ni(L^3H)_2]$	1M17	-7.7	0.006
	CDK2	-7.1	0.016
$[Cu(L^3H)_2]$	1M17	-8.2	0.009
	CDK2	-6.5	0.012

For the binding to EGFR target protein, the first three highest binding energies were determined in $[Cu(L^2H)_2]$ (-8.9kcal/mol), $[Ni(L^2H)_2]$ (-8.3kcal/mol) and $[Cu(L^3H)_2]$ (-8.2kcal/mol) complexes. Other compounds had lower binding energy values given in Table 1. Furthermore, the smallest inhibition constant which is related to the high potent of binding belongs to $[Cu(L^2H)_2]$ complex.

However, the binding energy values of the compounds with CDK2 target protein were lower than the EGFR's when compared. The highest binding energy value belongs to $[Cu(L^1H)_2]$ complex with -7.7kcal/mol. This result was supported by the inhibition constant value of $[Cu(L^1H)_2]$ which was the lowest one when compared to the others of CDK2.

Table 2. *Interaction types occurred between the compounds and target protein molecules*

	Target proteins					
	EGFR			**CDK2**		
Compound	**H-Bond**	**Hydrophobic**	**Electrostatic**	**H-Bond**	**Hydrophobic**	**Electrostatic**
L^1H_2	Lys721(3.289 Å) Lys721(2.831 Å) Asp831(2.473 Å)	Phe699(4.112 Å)	Glu738(5.335 Å) Asp831(4.433 Å) Asp831(4.161 Å) Asp831(3.952 Å) Asp831(4.112 Å) Phe699(4.871 Å)	Thr218(2.820 Å) Thr198(2.769 Å)	Leu202(5.293 Å)	-
$[Ni(L^1H)_2]$	Asp831(3.543 Å)	Lys855(5.039 Å)	Asp813(4.759 Å) Asp831(2.943 Å) Asp831(4.583 Å) Asp831(3.734 Å) Lys721(4.525 Å) Glu738(3.949 Å)	Thr198(3.085 Å) Thr218(3.010 Å) Val251(2.028 Å)	Pro253(5.477 Å) Arg217(4.005 Å)	-
$[Cu(L^1H)_2]$	Glu734(2.175 Å)	-	Asp831(5.520 Å) Asp831(4.982 Å) Asp831(4.288 Å) Asp813(4.939 Å) Glu734(4.313 Å)	Thr218(2.665 Å) Arg200(3.544 Å)	Pro254(5.124 Å) Arg217(5.176 Å)	-
L^2H_2	Glu738(1.959Å) Arg817(2.789Å)	-	Asp831(4.205 Å) Asp831(4.077 Å) Asp831(3.766 Å) Phe699(4.023 Å)	Thr182(2.950 Å) Arg274(1.938 Å)	-	-
$[Ni(L^2H)_2]$	Arg817(3.131 Å) Glu738(2.550 Å) Glu738(2.438 Å)	-	Asp813(5.576 Å) Asp831(4.863 Å) Asp831(4.215 Å)	Ala244(2.645 Å) Arg217(2.192 Å) Leu202(2.312 Å) Arg217(3.495 Å) Trp243(3.481 Å) Val251(3.766 Å) Gln246(4.197 Å)	Arg200(4.620 Å)	Arg200(4.889 Å)
$[Cu(L^2H)_2]$	Asp831(3.013 Å) Asp831(3.337 Å) Asp831(3.380 Å) Asn818(3.013 Å)	Ala731(5.318 Å)	Asp831(3.791 Å) Asp831(4.881 Å) Asp831(5.069 Å) Asp831(4.392 Å) Asp831(3.026 Å) Asp831(2.792 Å) Glu738(5.251 Å) Glu7343.649 Å)	Lys142(2.931 Å) Val29(2.181 Å) Ile63(1.923 Å)	Val29(3.885 Å) Lys65(3.830 Å)	
L^3H_2	Lys721(3.283 Å) Lys721(2.809 Å) Phe699(2.966 Å) Asp831(2.576 Å)	Phe699(4.177 Å) Val702(5.496 Å)	Glu738(5.368 Å) Asp831(4.225 Å) Asp831(3.967 Å) Asp831(4.090 Å) Phe699(4.821 Å)	Glu51(2.462 Å) Arg122(2.871 Å) Leu54(2.193 Å) Val123(3.440 Å)	Leu58(4.884 Å) His121(4.585 Å) Leu54(4.637 Å) Val123(5.307 Å)	Glu51(4.906 Å)
$[Ni(L^3H)_2]$	Asp831(3.583 Å) Ile854(4.009 Å)	Cys773(4.183 Å) Arg817(4.644 Å) Lys855(4.074 Å) Trp856(5.136 Å) Val702(5.414 Å) Pro853(4.925 Å) Ile854(5.356 Å) Ala896(5.267 Å)	Asp831(4.683 Å) Asp831(4.742 Å) Asp813(5.494 Å) Asp831(3.824 Å) Phe699(3.949 Å)	Thr182(3.034 Å) Ala277(2.980 Å) Ala116(2.430 Å) Phe117(3.557 Å) Ser120(3.589 Å)	Phe117(5.440 Å)	-
$[Cu(L^3H)_2]$	Lys721(2.949 Å) Phe699(2.314 Å)	Phe699(5.332 Å) Arg724(4.246 Å) Ala698(5.130 Å) Arg724(5.337 Å)	Glu734(5.556 Å) Asp831(4.206 Å) Asp831(3.778 Å)	Ser261(3.374 Å) Ser261(3.341 Å) Gln265(3.165 Å) Gln265(3.206 Å) Gln265(3.374 Å) Glu257(2.487 Å) His283(2.846 Å)	Ile275(4.746 Å) Pro284(5.012 Å)	Glu257(4.793 Å)

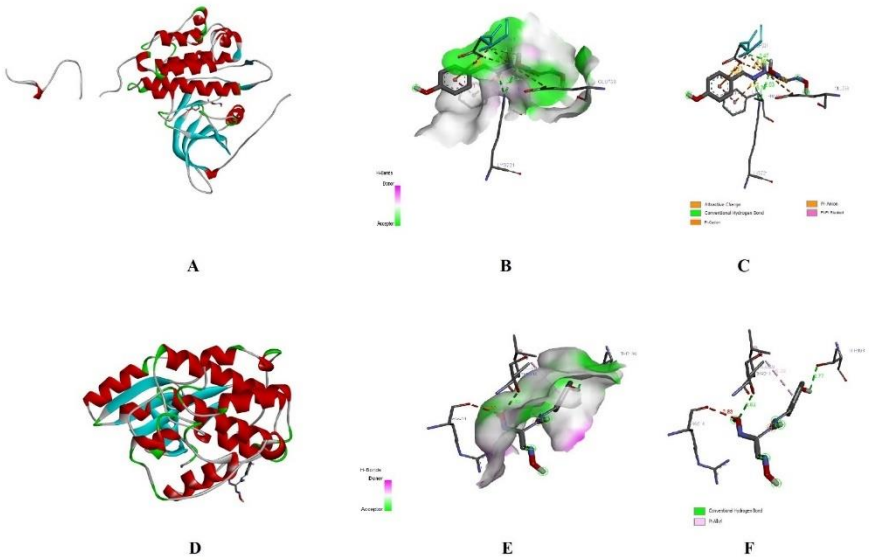

Figure 5. A, D) *3D diagram,* ***B, E)*** *2D diagram,*
C, F) *Hydrogen bonding interactions of L^1H_2 with EGFR and CDK2, respectively*

Figure 5 showed that L^1H_2 interacts with EGFR target protein through three conventional hydrogen bonds (Lys721, Asp831), one pi-pi stacked interaction (Phe699), three attractive charge interactions (Glu738, Asp831), one pi-cation (Phe699) and two pi-anion interactions (Asp831). Also, with CDK2 target protein, there were two conventional hydrogen bonds (Thr218, Thr198) and one pi-alkyl interaction (Leu202) occurred.

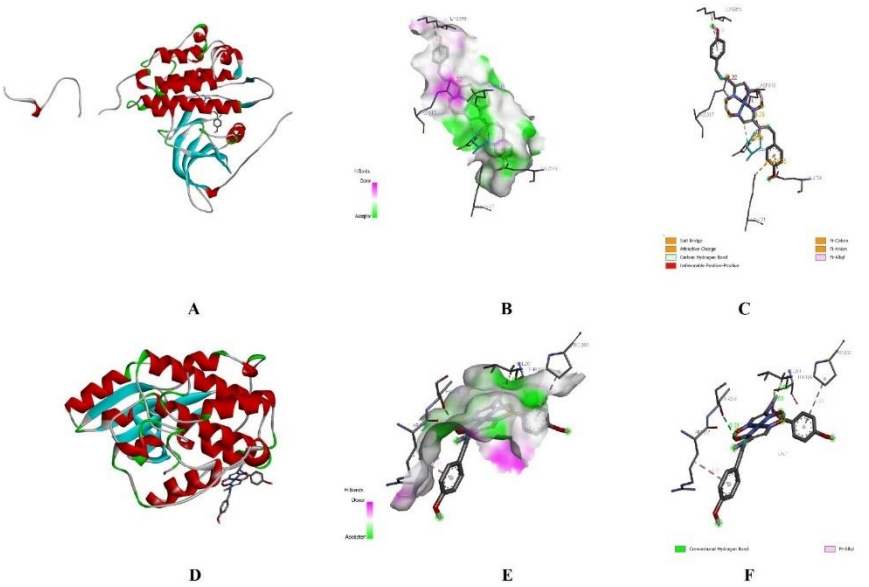

Figure 6. A, D) *3D diagram,* ***B, E)*** *2D diagram,*
C, F) *Hydrogen bonding interactions of $[Ni(L^1H)_2]$ with EGFR and CDK2, respectively*

In Figure 6, $[Ni(L^1H)_2]$ formed a conventional hydrogen bond with EGFR by Asp831 residue and had one pi-alkyl (Lys855), one salt bridge (Asp831), three attractive charge (Asp813, Asp831), one pi-cation (Lys721) and one pi-anion (Glu738) interactions with this target protein EGFR. Furthermore, $[Ni(L^1H)_2]$ had three conventional hydrogen bonds with Thr198, Thr218 and Val251 residues and had pi-alkyl interactions with Pro253 and Arg217 amino acids.

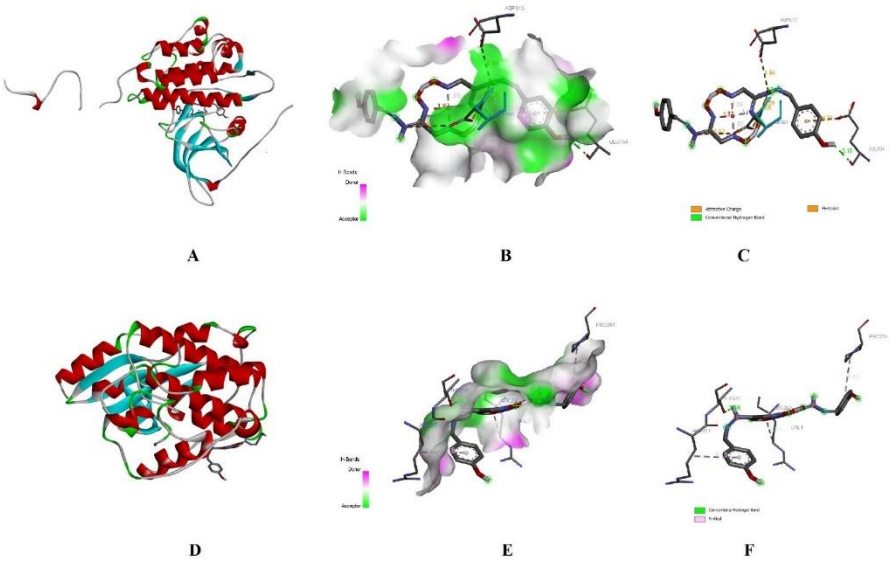

Figure 7. A, D) *3D diagram,* ***B, E)*** *2D diagram,*
C, F) *Hydrogen bonding interactions of [Cu(L^{1}H)$_2$] with EGFR and CDK2, respectively*

Figure 7 showed the interactions between [Cu(L^{1}H)$_2$] and target proteins EGFR and CDK2. [Cu(L^{1}H)$_2$] bound to Glu734 amino acid through a conventional hydrogen bond and had a pi-anion interaction. Furthermore, it formed three attractive charge interactions with Asp831 and one with Asp813 amino acids. Moreover, there was observed a conventional hydrogen bond with Thr218, carbon-hydrogen bond with Arg200, pi-alkyl interactions with Pro254 and Arg217 amino acids of CDK2 protein.

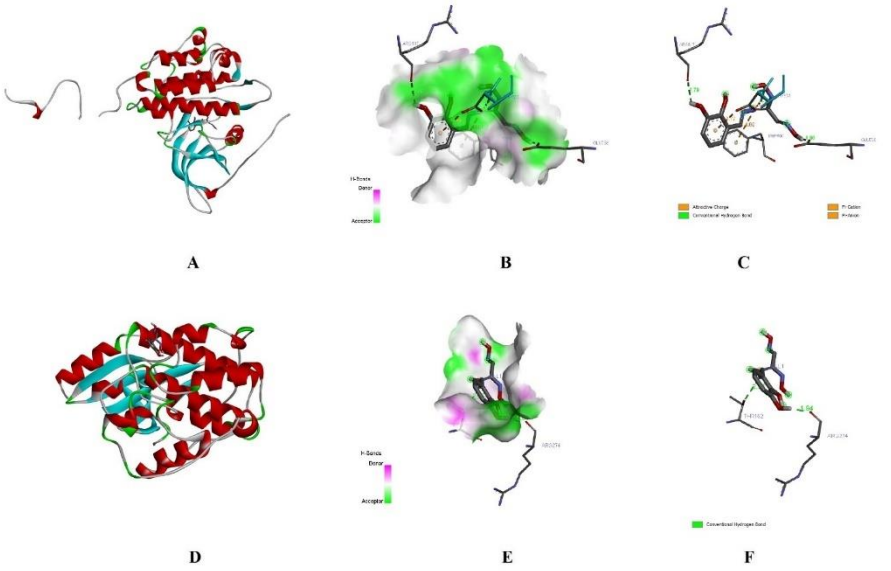

Figure 8. A, D) *3D diagram,* ***B, E)*** *2D diagram*
C, F) *Hydrogen bonding interactions of L^{2}H$_2$ with EGFR and CDK2, respectively*

There were two conventional hydrogen bonds occurred between L^{2}H$_2$ and Glu738 and Arg817 amino acids of EGFR target protein. Also, there were formed 2 attractive charge interactions and one pi-anion interaction with Asp831 and one pi-cation interaction with Phe699 amino acids (Figure 8A-C). Furthermore, L^{2}H$_2$ formed only two conventional hydrogen bonds with Thr182 and Arg274 amino acids of CDK2 target protein (Figure 8D-F).

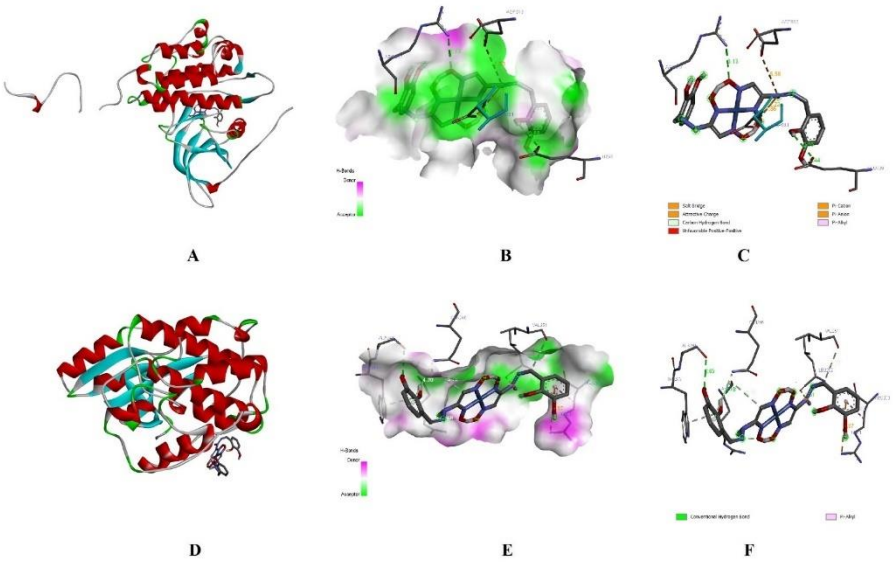

Figure 9. A, D) *3D diagram,* ***B, E)*** *2D diagram*
C, F) *Hydrogen bonding interactions of [Ni(L^{2}H)$_2$] with EGFR and CDK2, respectively*

In Figure 9 the interactions between the [Ni(L^{2}H)$_2$] complex and EGFR, CDK2 target proteins were shown. [Ni(L^{2}H)$_2$] interacted with Arg817 and Glu738 amino acids of EGFR by conventional hydrogen bonds and with Asp831 and Asp813 amino acids by attractive charge interactions. Furthermore, [Ni(L^{2}H)$_2$] formed three conventional hydrogen bonds with Ala244, Arg217 and Leu202 amino acids, four carbon-hydrogen bonds with Arg217, Trp243, Arg217 and Val251 amino acids, one pi-donor hydrogen bond with Gln246, one pi-cation and one pi-alkyl with Arg200 amino acid of CDK2.

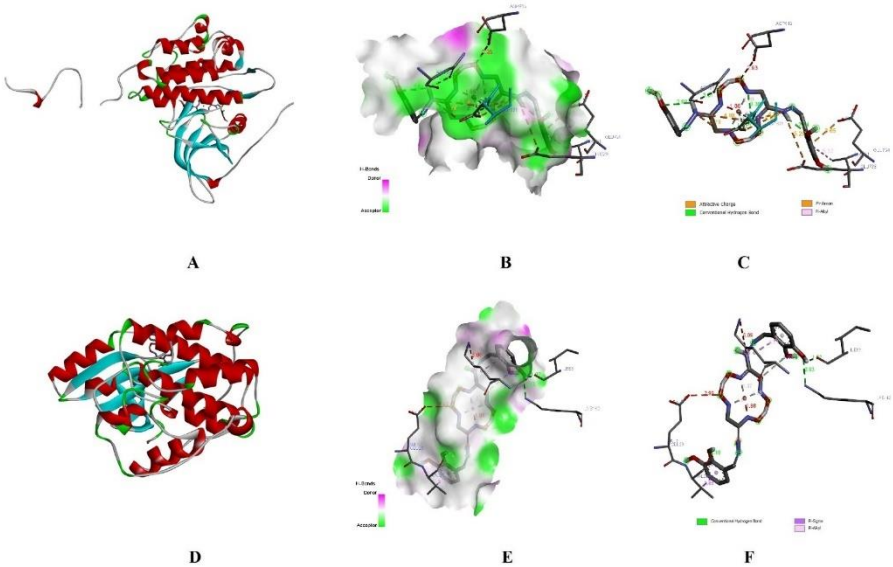

Figure 10. A, D) *3D diagram,* ***B, E)*** *2D diagram,*
C, F) *Hydrogen bonding interactions of [Cu(L^{2}H)$_2$] with EGFR and CDK2, respectively*

The interactions between [Cu(L^{2}H)$_2$] and EGFR were presented in Figure 10A-C. [Cu(L^{2}H)$_2$] was observed to form conventional hydrogen bonds three with Asp831 and one with Asn818 amino acids. Also, there were four attractive charge interactions with Asp831, one attractive charge interaction with Glu738, two metal acceptor interactions with Asp831, one pi-anion interaction with Glu734 and one pi-alkyl interaction with

Ala731 occurred. Moreover, $[Cu(L^2H)_2]$ formed three conventional hydrogen bonds with Lys142, Val29 and Ile63 amino acids of CDK2, one pi-sigma interaction with Val29 and one pi-alkyl interaction with Lys65 amino acids (Figure 10D-F).

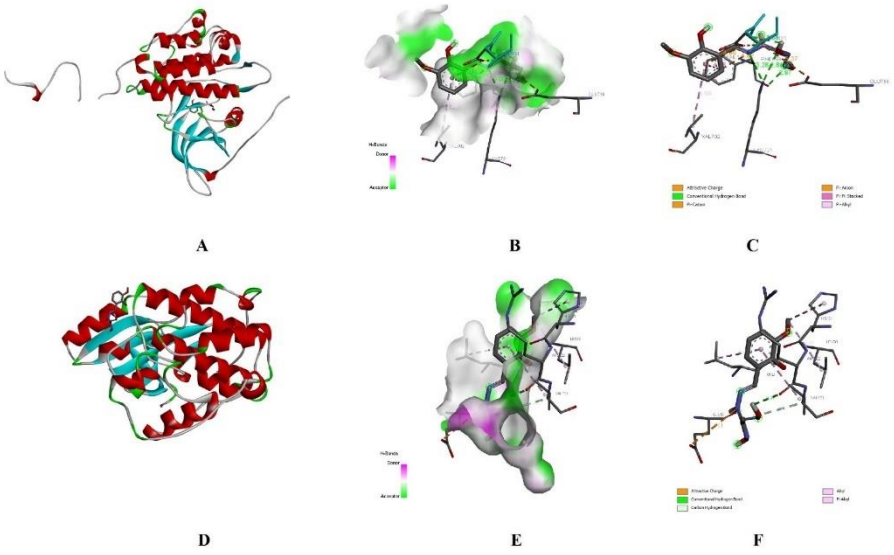

Figure 11. A, D) *3D diagram,* ***B, E)*** *2D diagram,*
C, F) *Hydrogen bonding interactions of L^3H_2 with EGFR and CDK2, respectively*

L^3H_2 formed one conventional hydrogen bond with Lys721 and Phe699 and two with Asp831. In addition, L^3H_2 interacted with Phe699 via pi-cation and pi-pi stacked interactions. It had pi-anion interaction with Asp831 and pi-alkyl interaction with Val702 amino acids (Figure 11A-C). Furthermore, there occurred conventional hydrogen bonds between L^3H_2 and Glu51, Arg122, Leu54 amino acids of CDK2 protein and one carbon-hydrogen bond with Val123, one alkyl interaction with Leu58, one attractive charge interaction with Glu51 and one pi-alkyl interaction with His121, Leu54 and Val123 amino acids (Figure 11D-F).

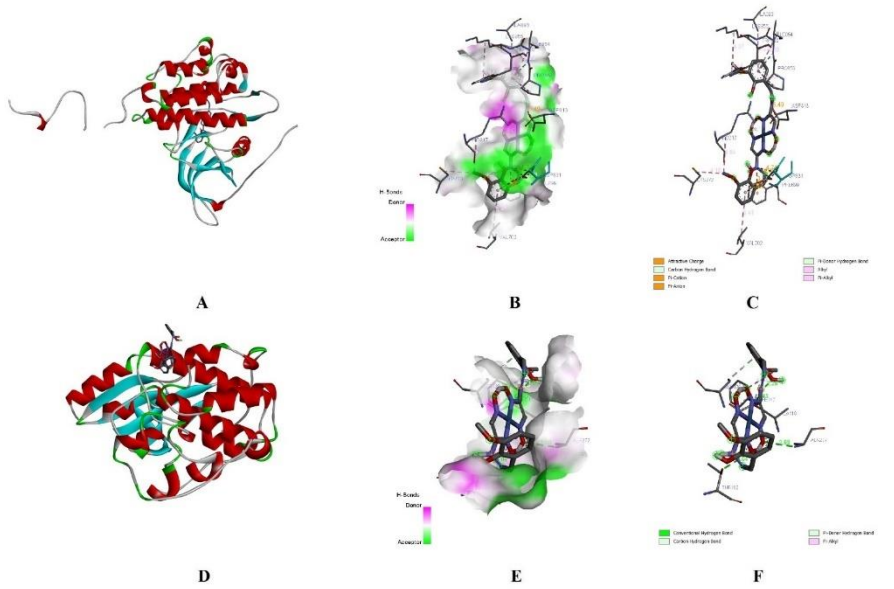

Figure 12. A, D) *3D diagram,* ***B, E)*** *2D diagram,*
C, F) *Hydrogen bonding interactions of $[Ni(L^3H)_2]$ with EGFR and CDK2, respectively*

$[Ni(L^3H)_2]$ had one carbon-hydrogen bond with Asp831 and pi-donor hydrogen bond with Ile854 amino acids of EGFR. Also, it had alkyl interactions with Cys773, Arg817, Lys855 amino acids, pi-alkyl interactions with Trp856, Val702, Pro853, Ile854, Ala896 amino acids, attractive charge interactions with Asp831 and Asp813 amino acids of EGFR (Figure 12A-C). Furthermore, it formed conventional hydrogen bonds with Thr182, Ala277 and Ala116, carbon-hydrogen bond with Phe117, pi-donor hydrogen bond with Ser120 and pi-alkyl interaction with Phe117 amino acids of CDK2 target protein (Figure 12D-F).

In Figure 13 there were presented the interactions between $[Cu(L^3H)_2]$ and target proteins EGFR and CDK2. Conventional hydrogen bonds were formed with Lys721 and Phe699 amino acids of EGFR. Also, there were one attractive charge interaction with Glu734, two pi-anion interactions with Asp831, one pi-pi stacked interaction with Phe699, one alkyl interaction with Arg724 and pi-alkyl interactions with Ala698 and Arg724 amino acids occurred. Moreover, there were formed conventional hydrogen bonds with Ser261, Gln265, Glu257 and His 283 amino acids, carbon-hydrogen bonds with Ser261 and Gln265 amino acids, alkyl interaction with Ile275, pi-alkyl interaction with Pro284 and attractive charge interaction with Glu257.

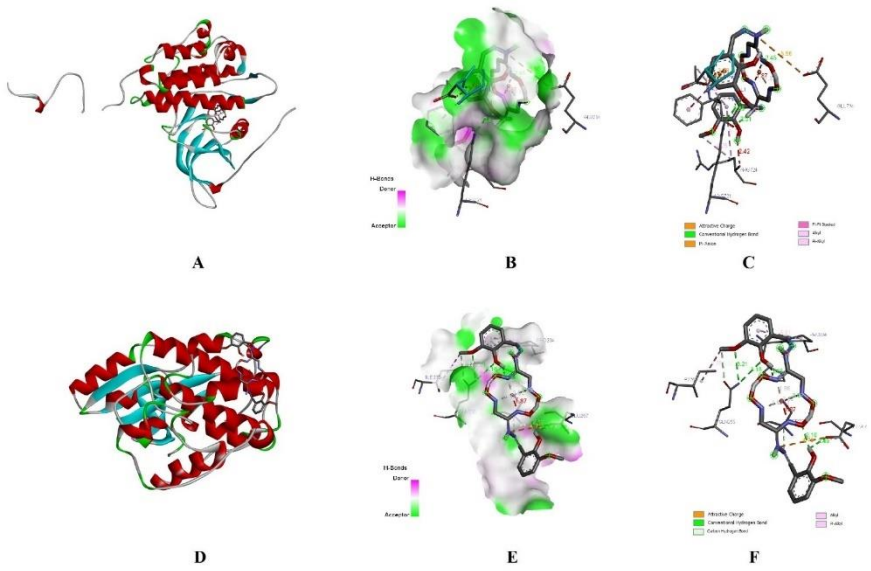

Figure 13. A, D) *3D diagram,* ***B, E)*** *2D diagram,*
C, F) *Hydrogen bonding interactions of* $[Cu(L^2H)_2]$ *with EGFR and CDK2, respectively*

3.3. Ligand Bioactivity

The bioactivity parameters LE and FQ results were given in Table 3 in detail. For approving the compound as a hit one, it must provide the conditions $LE \geq 0.3$, $FQ \geq 0.8$ (Sulaiman et al., 2019). $[Ni(L^2H)_2]$ and $[Cu(L^2H)_2]$ complexes with EGFR had the highest LE and FQ values and these were found to be in the recommended range. Furthermore, $[Cu(L^3H)_2]$ had an acceptable FQ value however its LE value was out of range. The results confirm the binding energy results where $[Ni(L^2H)_2]$, $[Cu(L^2H)_2]$ and $[Cu(L^3H)_2]$ had the highest binding scores against EGFR target protein.

Table 3. *Bioactivity results of L^1H_2, L^2H_2, L^3H_2 ligands and their Ni^{II} and Cu^{II} metal complexes*

Protein	Compound	Ligand Efficiency	LE scale	Fit Quality
EGFR	L^1H_2	0.400	0.512	0.781
	$[Ni(L^1H)_2]$	0.227	0.306	0.743
	$[Cu(L^1H)_2]$	0.212	0.306	0.693
	L^2H_2	0.376	0.497	0.757
	$[Ni(L^2H)_2]$	0.337	0.288	1.170
	$[Cu(L^2H)_2]$	0.354	0.288	1.229
	L^3H_2	0.350	0.483	0.725
	$[Ni(L^3H)_2]$	0.208	0.270	0.771
	$[Cu(L^3H)_2]$	0.222	0.270	0.821
CDK2	L^1H_2	0.325	0.512	0.635
	$[Ni(L^1H)_2]$	0.218	0.306	0.713
	$[Cu(L^1H)_2]$	0.233	0.306	0.763
	L^2H_2	0.324	0.497	0.651
	$[Ni(L^2H)_2]$	0.206	0.288	0.714
	$[Cu(L^2H)_2]$	0.217	0.288	0.754
	L^3H_2	0.317	0.483	0.656
	$[Ni(L^3H)_2]$	0.192	0.270	0.711
	$[Cu(L^3H)_2]$	0.176	0.270	0.651

3.4. Quantum Chemical Descriptors

ΔE_{gap} value specifies the conditions of the reactions. The kinetic stability of a molecule was determined by a high ΔE_{gap} value (Ferdous & Kawsar, 2020). In this case, the molecule is desperate to get more energy for jumping from the ground state to the exited one. The highest ΔE_{gap} value was found to belong to L^2H_2 and the lowest was the value of $[Cu(L^2H)_2]$ complex (Table 4). Furthermore, the lowest global hardness (η) and the highest global softness (σ) are related to the lowest ΔE_{gap} value (Allal et al., 2018). In our study, $[Cu(L^2H)_2]$ had the lowest η and the highest σ value when compared to other compounds. Besides, a high ω value corresponds to having a good electrophile property for a molecule (Rupa et al., 2022) where $[Cu(L^2H)_2]$ had the highest ω value in our study. Thus $[Cu(L^2H)_2]$ had a potent and sufficient electrophile ability (acceptor) among other compounds.

Table 4. *Quantum chemical calculation results*

Compounds	**E_{HOMO} (eV)**	**E_{LUMO} (eV)**	**ΔE_{gap} (eV)**	**χ**	**π**	**η**	**σ**	**ω**
L^1H_2	-0.209	0.399	0.608	-0.095	0.095	0.304	3.290	0.015
$[Ni(L^1H)_2]$	-0.273	-0.211	0.062	0.242	-0.242	0.031	32.363	0.945
$[Cu(L^1H)_2]$	-0.210	-0.201	0.009	0.205	-0.205	0.004	243.902	5.145
L^2H_2	-0.292	0.328	0.620	-0.177	0.018	0.310	3.231	0.001
$[Ni(L^2H)_2]$	-0.274	-0.212	0.062	0.243	-0.243	0.031	32.258	0.949
$[Cu(L^2H)_2]$	-0.208	-0.200	0.008	0.204	-0.204	0.004	250.000	5.202
L^3H_2	-0.222	0.380	0.602	-0.079	0.079	0.301	3.323	0.010
$[Ni(L^3H)_2]$	-0.272	-0.209	0.064	0.240	-0.240	0.032	31.104	0.898
$[Cu(L^3H)_2]$	-0.209	-0.198	0.010	0.204	-0.204	0.005	194.175	4.023

4. CONCLUSION

Molecular docking, bioactivity and quantum chemical properties of vic-Dioxim derivatives bearing hydrazone group and their Ni^{II} and Cu^{II} complexes were analysed. Ni^{II} and Cu^{II} complexes of the L^1H_2, L^2H_2 and L^3H_2 ligands showed higher binding affinity to EGFR and CDK2. Especially, $[Cu(L^1H)_2]$ and $[Cu(L^2H)_2]$ complexes can be suggested as hit compounds against CDK2 and EGFR, respectively. These were supported by the inhibition constant values which were the lowest when compared to others. L^1H_2, L^2H_2 and L^3H_2 ligands had the lowest binding energy values when compared to metal complexes. Also, $[Cu(L^2H)_2]$ complex had a high binding energy value against EGFR. $[Ni(L^2H)_2]$ and $[Cu(L^2H)_2]$ complexes with EGFR had the highest LE and FQ values. Furthermore, $[Cu(L^2H)_2]$ had a potent and sufficient electrophile ability (acceptor) among other compounds. Therefore, these compounds may be suitable compounds for further analysis in anti-cancer drug development with low toxic and targeted properties.

ACKNOWLEDGEMENT

The authors received no financial support for this study.

CONFLICT OF INTEREST

The authors declare no conflict of interest.

REFERENCES

Accelrys. (2014). Discovery Studio Visualizer Software. San Diego, CA: Accelrys.

Allal, H., Belhocine, Y., & Zouaoui, E. (2018). Computational study of some thiophene derivatives as aluminum corrosion inhibitors. *Journal of Molecular Liquids*, *265*, 668-678. doi:10.1016/j.molliq.2018.05.099

Altamimi, A. S., El-Azab, A. S., Abdelhamid, S. G., Alamri, M. A., Bayoumi, A. H., Alqahtani, S. M., Alabbas, A. B., Altharawi, A. I., Alossaimi, M. A., & Mohamed, M. A. (2021). Synthesis, Anticancer Screening of Some Novel Trimethoxy Quinazolines and VEGFR2, EGFR Tyrosine Kinase Inhibitors Assay; Molecular Docking Studies. *Molecules*, *26*, 2992. doi:10.3390/molecules26102992

Canpolat, E., & Kaya, M. (2005). Synthesis and formation of a new vic-dioxime complexes. *Journal of Coordination Chemistry*, *58*(14), 1217-1224. doi:10.1080/00958970500130501

DeLano, W. L. (2013). The PyMOL Molecular Graphics System. San Carlos, CA: DeLano Scientific LLC. URL

Ferdous, J., & Kawsar, S. M. A. (2020). Thermochemical, Molecular Docking and ADMET Studies of Some Methyl α-D-Glucopyranoside Derivatives. *The Chittagong University Journal of Science*, *42*(1), 58-83. doi:10.3329/cujs.v42i1.54238

Fouad, R., & Adly, O. M. I. (2021). Novel Cu^{2+} and Zn^{2+} nanocomplexes drug based on hydrazone ligand bearings chromone and triazine moieties: Structural, spectral, DFT, molecular docking and cytotoxic studies. *Journal of Molecular Structure*, *1225*, 129158. doi:10.1016/j.molstruc.2020.129158

Haider, K., Rehman, S., Pathak, A., Najmi, A. K., & Yar, M. S. (2021). Advances in 2-substituted benzothiazole scaffold-based chemotherapeutic agents. *Archiv der Pharmazie*, *354*(12), e2100246. doi:10.1002/ardp.202100246

Horchani, M., Della Sala, G., Caso, A., D'Aria, F., Esposito, G., Laurenzana, I., Giancola, C., Costantino, V., Jannet, H. B., & Romdhane, A. (2021). Molecular Docking and Biophysical Studies for Antiproliferative Assessment of Synthetic Pyrazolo-Pyrimidinones Tethered with Hydrazide-Hydrazones. *International Journal of Molecular Sciences*, *22*, 2742. doi:10.3390/ijms22052742

Knizia, G. (2022) IboView, Version 20150427, http://www.iboview.org, Accessed: 18/072022

Koopmans, T. (1934). Über die Zuordnung von Wellenfunktionen und Eigenwerten zu den einzelnen Elektronen eines Atoms. *Physica*, *1*(1-6), 104–113. doi:10.1016/S0031-8914(34)90011-2

Kurtoglu, M., & Baydemir, S.A. (2007). Studies on Mononuclear Transition Metal Chelates Derived from a Novel (E, E)-Dioxime: Synthesis, Characterization and Biological Activity. *Journal of Coordination Chemistry*, *60*(6), 655-665. doi:10.1080/00958970600896076

Park, H.-J., Lee, K., Park, S.-J., Ahn, B., Lee, J.-C., Cho, H., & Lee, K.-I. (2005). Identification of Antitumor Activity of Pyrazole Oxime Ethers. *Bioorganic and Medicinal Chemistry Letters*, *15*(13), 3307-3312. doi:10.1016/j.bmcl.2005.03.082

Rija, A., Bulhac, I., Coropceanu, E., Gorincioi, E., Calmîc, E., Barba, A., & Bologa, O. (2011). Synthesis and Spectroscopic Study of some Coordinative Compounds of Co(III), Ni(II) and Cu(II) with Dianiline- and Disulfanilamideglyoxime. *Chemistry Journal of Moldova*, *6*(2), 73-78. doi:10.19261/cjm.2011.06(2).16

Rupa, S. A., Moni, M. R., Patwary, M. A. M., Mahmud, M. M., Haque, M. A., Uddin, J., & Abedin, S. M. T. (2022). Synthesis of Novel Tritopic Hydrazone Ligands: Spectroscopy, Biological Activity, DFT, and Molecular Docking Studies. *Molecules*, *27*(5), 1656. doi:10.3390/molecules27051656

Sarikavakli, N., & Irez, G. (2005). Synthesis and Complex Formation of Some Novel vicDioxime Derivatives of Hydrazones. *Turkish Journal of Chemistry*, *29*(1), 107-116.

Sarikavakli, N., & Cakici, H. T. (2012). Synthesis and Characterization of Novel (Z, E)-vic-dioximes and their Transition Metal Complexes. *Asian Journal of Chemistry*, *24*(3), 2643.

Serin, S. (2001). New vic-dioxide transition metal complexes. *Transition Metal Chemistry*, *26*(3), 300-306. doi:10.1023/A:1007163418687

Smith, A. G., Tasker, P. A., & White, D. J. (2003). The Structures of Phenolic Oximes and their Complexes. *Coordination Chemistry Reviews*, *241*(1-2), 61-85. doi:10.1016/S0010-8545(02)00310-7

Soga, S., Sharma, S., Shiotsu, Y., Shimizu, M., Tahara, H., Yamaguchi, K., Ikuina, Y., Murakata, C., Tamaoki, T., Kurebayashi, J., Schulte, T., Neckers L., & Akinaga, S. (2001). Stereospecific Antitumor Activity of Radicicoloxime Derivatives. *Cancer Chemotherapy Pharmacology*, *48*(6), 435-445. doi:10.1007/s002800100373

Sulaiman, K. O., Kolapo, T. U., Onawole, A. T., Islam, A., Adegoke, R. O., & Badmus, S. O. (2019). Molecular dynamics and combined docking studies for the identification of Zaire ebola virus inhibitors. *Journal of Biomolecular Structure and Dynamics*, *37*(12), 3029-3040. doi:10.1080/07391102.2018.1506362

Trott, O., & Olson, A. J. (2009). AutoDock Vina: Improving the speed and accuracy of docking with a new scoring function, efficient optimization, and multithreading. *The Journal of Computational Chemistry*, *31*, 455-461. doi:10.1002/jcc.21334

Tschugaeff, L. (1907). Über eine neue synthese der α-diketone. *European Journal of Inorganic Chemistry. 40*(1), 186-187. doi:10.1002/cber.19070400127